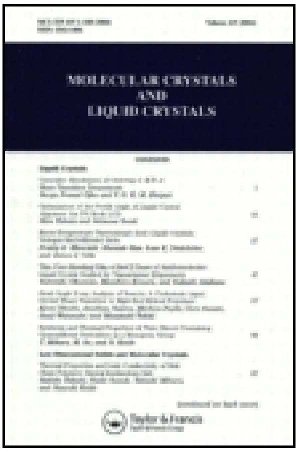

Molecular Crystals and Liquid Crystals
Publication details, including instructions for authors and subscription information:
http://www.tandfonline.com/loi/gmcl20

Electro-Optical Tuning in Photonic Crystals - Dispersed Liquid Crystalline Metamaterials

M. Rippa [a] , P. Mormile [a] , R. Capasso [a] , M. Zanella [b] & L. Petti [a]

[a] Institute of Cybernetics, National Research Council of Italy , Pozzuoli , (Naples) , Italy

[b] Fondazione Istituto Italiano di Tecnologia , Genova , Italy

Published online: 02 Apr 2013.

Mol. Cryst. Liq. Cryst., Vol. 573: pp. 18–25, 2013

ISSN: 1542-1406 print/1563-5287 online
DOI: 10.1080/15421406.2013.763333

Electro-Optical Tuning in Photonic Crystals – Dispersed Liquid Crystalline Metamaterials

M. RIPPA,[1] P. MORMILE,[1] R. CAPASSO,[1] M. ZANELLA,[2] AND L. PETTI[1,*]

[1]Institute of Cybernetics, National Research Council of Italy, Pozzuoli, (Naples), Italy
[2]Fondazione Istituto Italiano di Tecnologia, Genova, Italy

Two different metamaterial-liquid crystal structures are fabricated with the metamaterials as liquid crystal (LC) and semiconductor nanorods doped LC alignment layers. E-beam lithography was used to pattern the electron-sensitive polymer one-dimensional photonic crystal (PC) structures. The nanostructured aligning surfaces have been characterized by scanning electron microscopy. The PCs-Dispersed Liquid Crystalline Metamaterials have been investigated through polarized optical microscopy. The threshold voltage and response times for the undoped and doped nematic LCs in the glass cells are measured as a function of the applied external electric field.

Keywords Core-shell nanorods; electro-optical tuning; liquid crystals; metamaterials; photonic crystals

Introduction

Current research efforts on cutting-edge materials, such as photonic crystals (PCs), self-organizing nanomaterials, and polymeric and composite materials, are focused on obtaining novel or unique properties enabled by specialized molecular electronic, structural designs, or dopants. While most metamaterials developed to date consist of passive material constituents, several studies have emerged where material constituents containing electrooptics, nonlinear optics, or active (gain) material are involved [1–3]. Control and tuning of the metamaterial electromagnetic response are gaining research interests as a natural research development to attain functionality in metamaterials [4–6]. In a photonic device application, liquid crystal (LC) is the choice material when a control and tuning is pursued, as evidenced in wide applications to the optical display and photonic switching devices. On the other hand, one-dimensional (1D) semiconductor nanostructures are intriguing materials both for academic interest and industrial application. It has been shown that semiconductor nanowires own unique thermal, electric, optical, and mechanical properties, which have great potential applications, including novel solar cell architectures, nanolasers, communication, and biological science and technology [7–10]. To achieve a full potential for broader

*Address correspondence to L. Petti, Institute of Cybernetics, National Research Council of Italy, Via Campi Flegrei 34, I-80072 Pozzuoli, (Naples), Italy. E-mail: L.petti@cib.na.cnr.it, 0818675037

range of application, ways must be found to integrate them with existing technologies. In general, the incorporation of anisotropic nanoparticles in LCs has been investigated to achieve-long range alignment, large scale orientation manipulation, and for faster switching speed of LCs devices [11–13]. As an example Acharya et al. [14] found that nanorods (NRs) of proper dimension couple locally with the LC director field in a favorable energetic configuration which enhances long-range ordering and device performance. Chen et al. [12,15] showed that when CdSe NRs are embedded into a LC cell, NRs will align along the orientation of LCs molecules resulting in a very large emission anisotropy with a huge degree of polarization. The emission anisotropy can be easily manipulated by an external bias opening up new possible applications in polarized optoelectronic devices including integrated photonic devices, polarized light emitting diodes, flat panel displays, and many other chromogenic smart devices.

But, often the geometrical properties of the photonic structures give problems for controlling the alignment of the LC. In this article, we studied a reproducible way to create specific orientational order fields in LCs by means of novel nanostructured aligning surfaces. Two different metamaterial-LC structures are fabricated with the metamaterials as LC alignment layers. LC alignment was obtained in planar and twisted cells, doped and undoped, via top down technologies. E-beam lithography was used to pattern the electron-sensitive polymer 1D PC structures. The nanostructured aligning surfaces have been characterized by scanning electron microscopy (SEM). The PCs-Dispersed Liquid Crystalline Metamaterials (PCs-DLCMs) have been investigated through polarized optical microscopy (POM) and an electro-optic characterization.

Experimental

Fabrication

The core/shell CdSe/CdS NRs were prepared according to a procedure that was developed in a previously published work [16]. The average rod diameter and length, as determined by TEM were 4 and 50 nm (aspect ratio 12.5), respectively. These NRs are dispersed in the nematic LC E7 supplied by Merck. The samples were prepared using the standard steps for LC cell fabrications. In the substrates, a top-down fabrication process was introduced to nanostructure the aligning layers instead of using polymide rubbed alignment layers. Each clean indium tin oxide (ITO)-coated glass substrate with the dimensions of $1.5 \times 2\ cm^2$ was spin coated with the electron-sensitive styrene methyl acrylate based polymer (ZEP) at 3500 rpm for 30 s, then the surface-treated substrate was soft baked at 170°C for 5 min. After spin coating and soft baked, the nanopatterning with an area of $2 \times 2\ mm^2$ was impressed on the polymer film using electron beam lithography. Each substrate was then developed in *n*-Amyl acetate. The resulting 1D PC is made of a 1D air grating embedded into the polymer ZEP with each rectangular hole 600 nm wide, 2 mm long, and 100 nm thick, with 1.5 μm lattice pitch over an area of $2 \times 2\ mm^2$. The nanostructured polymer coated substrates serve as homogeneous planar alignment layers for surface LC molecules. Top and bottom nanostructured substrates were overlapped in the same 1D grating direction to form planar cells with an area of $2 \times 2\ mm^2$, and at 90° to form twisted aligned cells. Each cell was assembled putting 9-μm-thick Mylar spacers between two nanostructured substrates and gluing with epoxy resin from the outside. The cells were filled with the LC or with the NRs doped E7 at the isotropic temperature of the LCs. A schematic of the side-view structure of the samples is shown in Fig. 1.

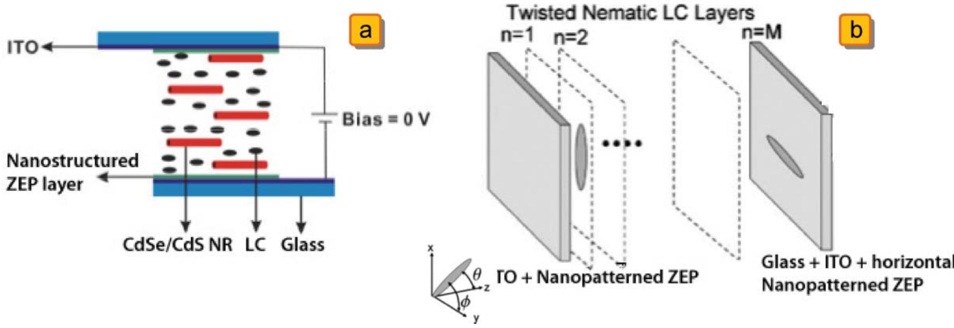

Figure 1. Schematic drawing of cell structures: (a) planar metamaterial-doped LC cell and (b) twisted metamaterial LC cell. The aligned area of the cell is 2×2 mm^2

Techniques

The experimental 1D PCs aligning layers realized have been characterized through SEM metrological measurements.

POM was employed in order to see the LC orientation in the cells.

The electro-optic characteristics of the planar metamaterial-LC cell structure have been investigated with the experimental setup reported by Khoo to measure birefringence and phase retardation of planar aligned nematic cells [17]. A He-Ne laser ($\lambda = 632.8$ nm) was used as light source and it was focused on the sample to explore only the aligned area of the cell. The linear polarizer was oriented at 45° with respect to the PC array direction (LC orientation direction) and the analyzer was crossed. This configuration gives the maximum phase retardation of the linearly polarized light impinging upon the aligned cell, due to different propagating speed of the extraordinary and ordinary rays in the LC medium. The transmission was measured by a photodiode detector and recorded digitally by a data acquisition system. An ac voltage square wave of 1 KHz was used to drive the LC cells whose inner sides were coated with ITO electrodes. Response times were also measured changing the frequency of a square wave and at a fixed applied voltage.

The twisted cells, doped and undoped, were characterized with the same experimental setup but with the polarizer oriented at 0° with respect to the PC array direction of the top substrate (LC optical axis at the top surface) and the analyzer was crossed.

Results and Discussion

Planar Metamaterial Doped and Undoped LC Cells

Figure 2 shows a SEM image of the 1D PC realized in the ZEP polymer.

The homogeneity of the planar alignment of the doped and undoped LC cells was checked with POM. The typical optical polarization microscope images are shown in Figs. 3(a) and (b) and 3(c) and (d) for the undoped and doped LC cells, respectively.

The pictures show the strong alignment effect of the gratings on the LC layer. The orientation of the molecules at the surfaces adapt to the minimal energy configuration forced by the grating on both sides. The alignment is along the grating direction (i.e., along the sides of the rectangular holes). Despite the presence of the CdSe/CdS NRs dispersed in the LC, these last ones seem to be planarly aligned as expected by the metamaterials

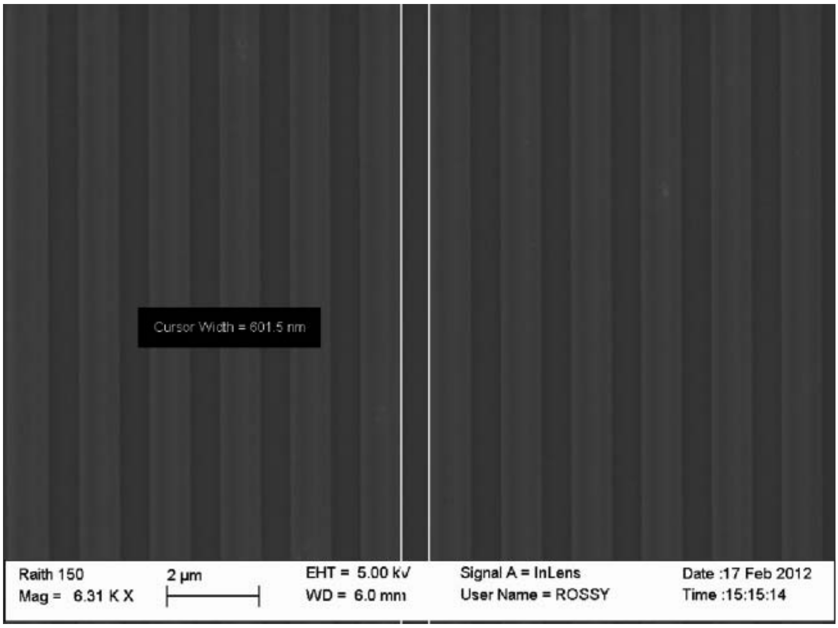

Figure 2. SEM image of the 1D PC obtained arranging rectangular air holes into the polymer (long 2 mm, wide $d = 600$ nm and lattice constant $a = 1.5$ μm).

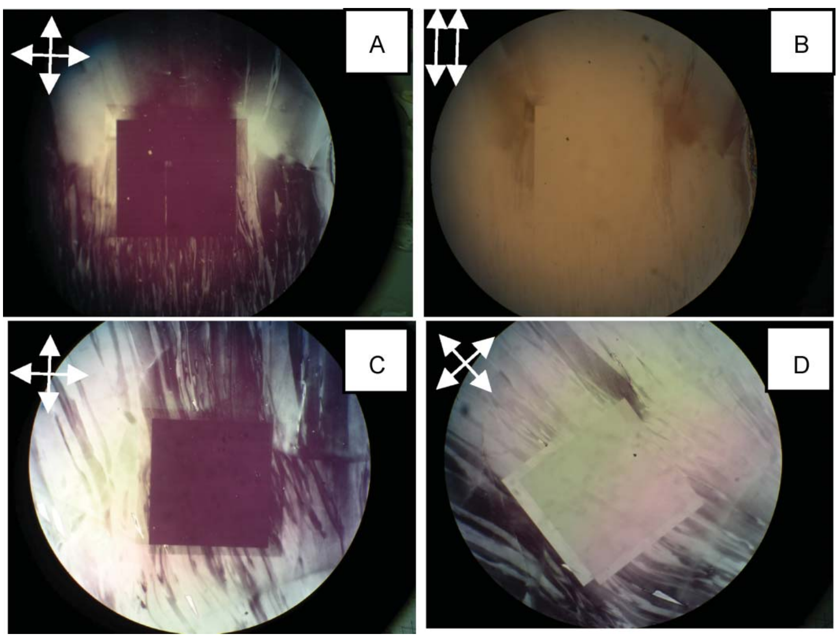

Figure 3. Optical Polarization Microscope images for the planar PCs-DLCMs in an undoped (a and b) and doped cell (c and d), respectively. The white arrows show the directions of polarizer and analyzer.

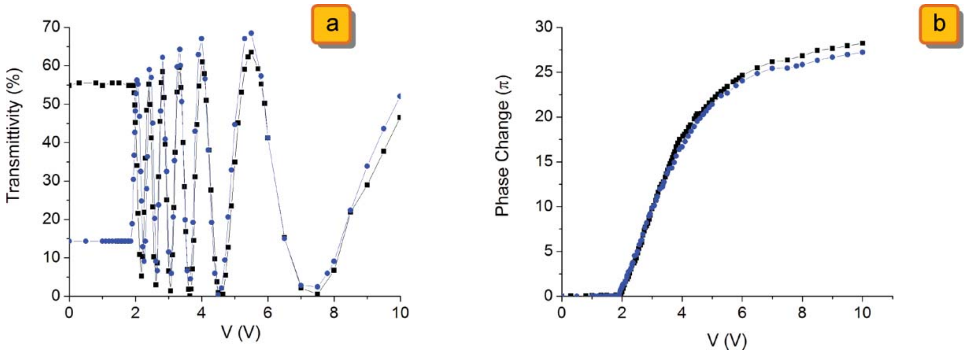

Figure 4. (a) Voltage-dependent transmission of a homogeneous 9-μm PCs-DLCMs in the LC cell (square dot curve) and in the cell filled with CdSe/CdS NRs-doped E7 (circle dot curve) at 1 kHz of the external applied field. (b) Voltage-dependent phase change when a 1 kHz square wave is applied to the cells. The threshold voltage V_{th} is, in this case extrapolated to be equal to 1.9 V.

patterned on top and down substrates. In these structures, the semiconductor NRs can form a well-aligned array with the assistance of LCs [12,15]: the embedded NRs will align with LC molecules along the grating direction due to the surface coupling between LC molecules and NRs. Further studies to verify such behavior are in progress.

In Figs. 4(a) and (b) is reported the transmittivity and the phase change versus the applied voltage for the undoped and doped cells. The transmitted light intensity through the polarizer-cell-analyzer system is related to the phase retardation δ as follows [17]:

$$T = \sin^2(\delta/2) \tag{1}$$

The phase retardation occurs due to the different propagating velocity of the ordinary and extraordinary rays in the LC film:

$$\delta(V, T, \lambda) = 2\pi d \Delta n(V, T, \lambda)/\lambda \tag{2}$$

where d is the cell thickness, Δn is the effective LC birefringence, T is the temperature, and λ is the wavelength. The phase retardation induced by the aligned part of the cell can be calculated from the voltage-dependent transmitted intensity. In order to calculate the threshold voltage (Freedericksz voltage), we plot the phase change $\Delta\varphi = \delta_{max} - \delta$ as a function of voltage and we do a linear extrapolation near the threshold region [17], as shown in Fig. 4(b).

We evaluated the Freedericksz threshold voltage which occurs at $V = 1.9$ V for both planar PCs-DLCMs, undoped and doped. In such a situation, when the applied voltage is lower than a threshold value (approximately 1.9 Vpp), no distortion induced in the LC molecular director appears. When the voltage is increased above the threshold, the reorientation of NLC molecules occurs: for positive dielectric anisotropy, the molecules are forced to be aligned from planar to homeotropic and transmission drops down.

In Figs. 5(a) and (b) we report the response times of the PCs-DLCMs in the cells when a 1 Hz square wave is applied to the cells at a fixed external applied voltage $V = 11$ V. The response times were estimated to be $\tau_{ON} = 56$ ms and decay time $\tau_{OFF} = 107$ ms for the PCs-DLCMs in the undoped LC cell and $\tau_{ON} = 7$ ms and $\tau_{OFF} = 9$ ms for the PCs-DLCMs in the cell filled with CdSe/CdS NRs-doped E7.

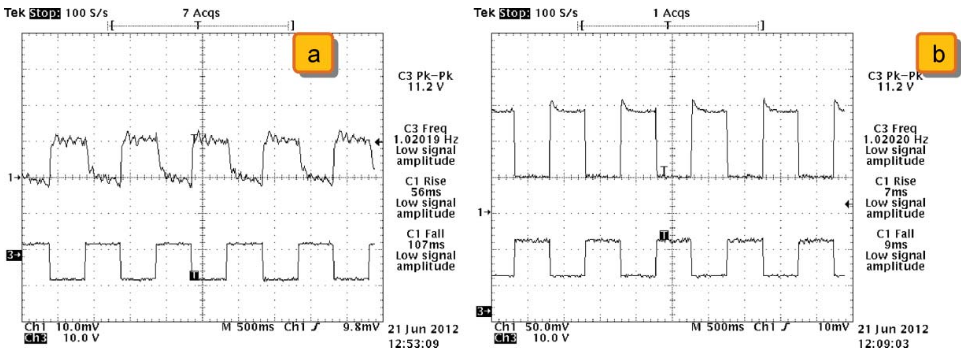

Figure 5. Response times of the PCs-DLCMs in the cells when a 1 Hz square wave is applied to the cells at a fixed external applied voltage $V = 11$ V. (a) Rise time $\tau_{ON} = 56$ ms and decay time $\tau_{OFF} = 107$ ms for the PCs-DLCMs in the LC cell. (b) $\tau_{ON} = 7$ ms and $\tau_{OFF} = 9$ ms for the PCs-DLCMs in the cell filled with CdSe/CdS NRs-doped E7.

Twisted Metamaterial Doped and Undoped LC Cell

Optical polarization microscope images are shown in Figs. 6(a) and (b) and 6(c) and (d) for the PCs-DLCMs in the undoped and doped LC cells, respectively.

Also in this cell structure, the pictures show the strong alignment effect of the gratings on the LC layer. The alignment is along the grating direction (i.e., along the sides of the rectangular holes) as schematically reported in Fig. 1(b) for both undoped and

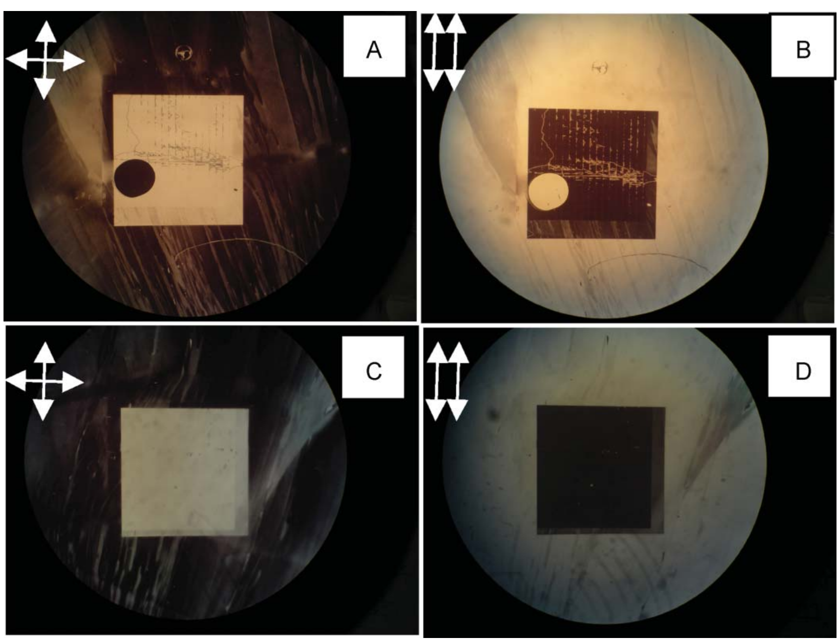

Figure 6. Optical polarization microscope images for the twisted PCs-DLCMs in an undoped (a and b) and doped cell (c and d), respectively. The white arrows show the directions of polarizer and analyzer.

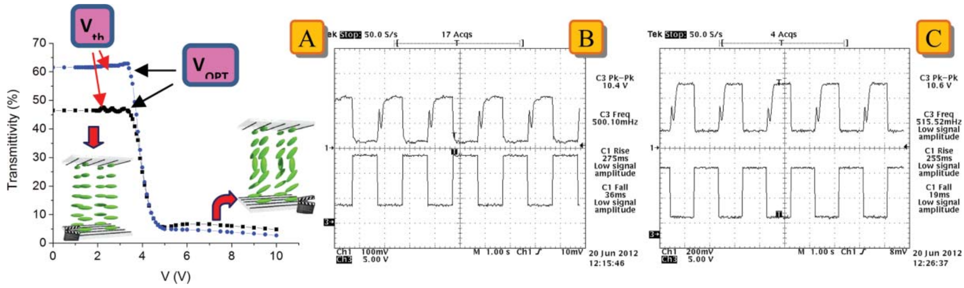

Figure 7. (a) Voltage-dependent transmission of a homogeneous 9-μm twisted PCs-DLCMs in the LC cell (square dot curve) and in the doped cell (circle dot curve) at 1 kHz of the external applied field. (b and c) Response times of the twisted PCs-DLCMs in the cells when a 500 mHz square wave is applied to the cells at a fixed external applied voltage $V = 11$ V. (b) Rise time $\tau_{ON} = 275$ ms and decay time $\tau_{OFF} = 36$ ms for the PCs-DLCMs in the LC cell. (c) $\tau_{ON} = 255$ ms and $\tau_{OFF} = 19$ ms for the PCs-DLCMs in the cell filled with CdSe/CdS NRs-doped E7.

doped cells. It is worth noting that the strong anchoring condition corresponds to the areas where the two patterned substrates (top and bottom) overlap. The shadow areas visible on the borders are due to a non perfect overlapping of the gratings which correspond to only one top alignment layer for those specific areas resulting in a weaker anchoring condition.

In Figs. 7(a)–(c), we reported the transmittivity and the response times versus the applied voltage for the undoped and doped cells. If the intensity of the light is low and does not induce appreciable changes in the birefringence of the LC, the Mauguin criterion applies () and the polarization of the transmitted light will rotate from the x to the y direction by the LC $\Delta nd \gg \lambda$ cell (see Fig. 1), following the Mauguin theorem. The transmission through the exit polarizer is, therefore, at the maximum.

The Freedericksz threshold voltage occurs at $V = 2.3$ V for both twisted PCs-DLCMs, undoped and doped. When the voltage is increased above the optical threshold V_{OPT}, the LC molecules are forced to be aligned from planar to homeotropic and transmission through crossed polarizers drops down [17].

In Figs. 7(b) and (c), we report the response times of the twisted PCs-DLCMs in the cells when a 500 mHz square wave is applied to the cells at a fixed external applied voltage $V = 11$ V. The response times were estimated to be $\tau_{ON} = 275$ ms and decay time $\tau_{OFF} = 36$ ms for the PCs-DLCMs in the undoped LC cell and $\tau_{ON} = 255$ ms and $\tau_{OFF} = 19$ ms for the PCs-DLCMs in the cell filled with CdSe/CdS NRs-doped E7.

Conclusions

In summary, we studied a reproducible way to create specific orientational order fields in LCs by means of novel nanostructured aligning surfaces. By employing 1D polymer metamaterials as the alignment layers two metamaterial-LC cell structure are fabricated: planar and twisted. The LC has been doped with semiconductor CdSe/CdS core/shell NRs in view of further studies of getting a well aligned array of semiconductor NR with the assistance of LCs. Response times for the planar doped metamaterial-LC structure are faster ($\tau_{ON} = 7$ ms and $\tau_{OFF} = 9$ ms) compared to those of the undoped system.

References

[1] Werner, D. H., Kwon, D.-H., Khoo, I. C., Kildeshev, A. V., & Shalaev, V. M. (2007). *Opt. Exp.*, *15*, 3342–3347.
[2] Khoo, I. C., Werner, D. H., Liang, X., Diaz, A., & Weiner, B. (2006). *Opt. Lett.*, *31*, 2592–2594.
[3] Govyadinov, A. A., Podolskiy, V. A., & Noginov, M. A. (2007). *Appl. Phys. Lett.*, *91*, 191103-1-191103-3.
[4] Zheludev, N. I. (2010). The road ahead for metamaterials. *Science*, *328*, 582.
[5] Khoo, I. C., Diaz, A., Liou, J., Stinger, M. V., Junbin Huang, & Yi Ma. (2010). *IEEE J. Sel. Top. Quant. Electron.*, *16*, 410–417.
[6] Petti, L., Rippa, M., Zhou, J., Manna, L., & Mormile, P. (2011). *Nanotechnology*, *22*, 285–307.
[7] Scholes, G. D. (2008). *Adv. Funct. Mater.*, *18*, 1157–1172.
[8] Kislyuk, V. V., & Dimitriev, O. P. (2008). *J. Nanosci. Nanotechnol. 8*, 131–148.
[9] Cozzoli, P. D., Pellegrino, T., & Manna, L. (2006). *Chem. Soc. Rev.*, *35*, 1195–1208.
[10] Zavelani-Rossi, M., Lupo, M. G., Krahne, R., Manna, L., & Lanzani, G. (2010). *Nanoscale*, *35*, 931.
[11] Yada, M., Yamamoto, J., & Yokoyama, H. (2004). *Phys. Rev. Lett.*, *92*, art. n. 185501.
[12] Wu, K. J., Chu, K. C., Chao, C. Y., Chen,Y. F., Lai, C. W., Kang, C.C., Chen, C. Y., & Pi-Tai Chou, P. T. (2007). *Nano Lett.*, *7*, 1908–1913.
[13] Skarabot, M., Ravnik, M., Zumer, S., Tkalec, U., Poberaj, I., Babic, D., & Musevic, I. (2008). *Phys. Rev. E*, *77*, 061706.
[14] Acharya, S., Kundu, S., Hill, J. P., Richards, G. J., & Ariga, K. (2009). *Adv. Mater.*, *21*, 989–993.
[15] Chen, H. S., Chen, C. W., Wang, C. H., Chu, F. C., Chao, C. Y., Kang, C. C., Chou, P. T., & Chen, Y. F. (2010). *J. Phys. Chem. C*, *114*(17), 7995–7998.
[16] Carbone, L., Nobile, C., De Giorgi, M., Della Sala, F., Morello, G., Pompa, P., Hytch, M., Snoeck, E., Fiore, A., Franchini, I. R., Nadasan, M., Silvestre, A. F., Chiodo, L., Kudera, S., Cingolani, R., Krahne, R., & Manna, L. (2007). *Nano Lett.*, *7*, 2942–2950.
[17] Khoo, I. C., & Wu, S. T. (1993). *Optics and Nonlinear Optics of Liquid Crystals World Scientific*, Singapore, Chap. 2.